

Observations of a Hybrid Double-Streamer/Pseudostreamer in the Solar Corona

L. A. Rachmeler¹, S. J. Platten², C. Bethge³, D. B. Seaton¹, and A. R. Yeates⁴

¹Royal Observatory of Belgium, Avenue Circulaire 3, 1180 Brussels, Belgium

²School of Mathematics and Statistics, University of St. Andrews, North Haugh, St. Andrews, Fife KY16 9SS, UK

³Kiepenheuer-Institut für Sonnenphysik, Schöneckstr. 6, 79104 Freiburg, Germany

⁴Department of Mathematical Sciences, Durham University, Science Laboratories, South Road, Durham DH1 3LE, UK

rachmeler@oma.be

Received _____; accepted _____

ABSTRACT

We report on the first observation of a single hybrid magnetic structure that contains both a pseudostreamer and a double helmet streamer. This structure was originally observed by the SWAP instrument aboard the PROBA2 satellite between 5 and 10 May 2013. It consists of a pair of filament channels near the south pole of the sun. On the western edge of the structure, the magnetic morphology above the filaments is that of a side-by-side double helmet streamer, with open field between the two channels. On the eastern edge, the magnetic morphology is that of a coronal pseudostreamer without the central open field. We investigated this structure with multiple observations and modelling techniques. We describe the topology and dynamic consequences of such a unified structure.

Subject headings: Sun: corona, Sun: filaments, prominences, Sun: magnetic fields

1. Introduction

Streamer-like structures have been studied for many years, and there are two general categories of features that fall into this classification: streamers and pseudostreamers/unipolar streamers (Pneuman & Kopp 1971; Wang et al. 2007). They are often identified by their upper-coronal white-light signatures, which are both extended bright radial features. Although these radial patterns are slightly different, it is the magnetic morphologies that truly distinguish the two types of structures. Those morphologies cannot be pinpointed with white-light measurements, partially due to the spatial gap in data coverage, but also because the measurements are sensitive to density, rather than magnetic field. Similarly, coronal EUV imagers record properties of the plasma, which follows the magnetic field, but are not directly sensitive to it.

In this letter, we focus specifically on the magnetic properties of the two different morphologies. For clarity, and because the definitions vary slightly in the current literature, we define the two structures as follows: A coronal *streamer* is a magnetic structure overlying a single (or an odd number of) polarity inversion lines (PILs) with closed loops in the lower corona and oppositely oriented open magnetic field in the upper corona, such that a current sheet and plasma sheet are present between the two open field domains. A *pseudostreamer* is a magnetic structure overlying two (or an even number of) PILs such that above the closed field, two domains of open field of the same polarity come together and no current sheet is present.

We present the first identification of a single hybrid magnetic structure composed of both a side-by-side double streamer (DS) and a pseudostreamer (PS). The transition between the two morphologies occurs in space, rather than in time, such that both exist simultaneously within a coherent structure that changes along its length. The change of magnetic topology has implications for the stability of the enclosed filament channels, and

the solar wind properties of the system.

Pseudostreamers can be very long lived. We observed a PS in the southern hemisphere of the sun that persisted from at least mid-2012 until mid-2013. This structure can be seen in PROBA2/SWAP movies, rotating in and out of the plane-of-sky (see Figure 5 by Seaton et al. 2013a). The PS is generally only visible for part of the rotation, although one or both of the individual filament channels can extend beyond the region where the PS topology is present. In the case where both filament channels extend beyond the PS, it is possible for the PS to split into a DS.

We have observed an example of just this type of topological change. Near the leading edge of the long-lived PS discussed above, we observed a DS that persisted for several rotations. In this letter we present these observations during Carrington rotation 2136 in May 2013. We also present simulated observations of simple magnetic models that support our interpretation of this structure.

2. Magnetic models and morphology

Double streamers and pseudostreamers are similar, but topologically distinct, magnetic structures. Figure 1A and 1B shows these two magnetic configurations and their magnetic skeletons (Parnell et al. 2008). Both models are simple axisymmetric potential field source surface (PFSS) extrapolations from a photospheric boundary magnetic field calculated using spherical harmonics, and do not contain longitudinal field.

In the 2D cross section of the DS model shown in Figure 1A, there are two null points at the upper source surface (marked by stars). Each null point forms the upper tip of a cusp-shaped separatrix (dashed lines) that encloses each closed loop volume below it. A trumpet-shaped volume of open field is sandwiched between the two closed-field volumes,

and is of opposite polarity to the polar open field.

Unlike in a DS, in a PS there is no open field between the closed field volumes that straddle the two PILs. Instead, in 2D, the separatrices that bound the two closed field regions meet at a single null. Outside of the closed field regions in the PS model, there are two open field domains of like polarity. These open field domains meet above the null point and are separated by the spine of the null. The spine also extends downward from the null to separate the two closed field regions from one another. In Figure 1B, the spines are shown with a dash-dot line and the separatrices are dashed.

A DS and a PS can be combined into a single hybrid structure with two continuous PILs. The transition from a DS to a PS is accomplished by the narrowing of the distance between the two separate DS null-lines until they meet and merge into a single null. A decrease of magnetic field strength of the central polarity between the two PILs on the photosphere could cause this narrowing. Figure 2 qualitatively shows how this might occur in 3D by illustrating longitudinal cuts in a highly simplified toy model of the system.

While our models capture the basic characteristics and skeleton of the magnetic configurations, when present on the sun, such structures would have a more complex topology. PILs on the sun are rarely perfectly straight, currents are practically ubiquitous, and the structure would be influenced by external features such as active regions. Titov et al. (2012) present a detailed topological description of several complex PSs which shows how these simple magnetic structures quickly become quite complex in a more realistic environment.

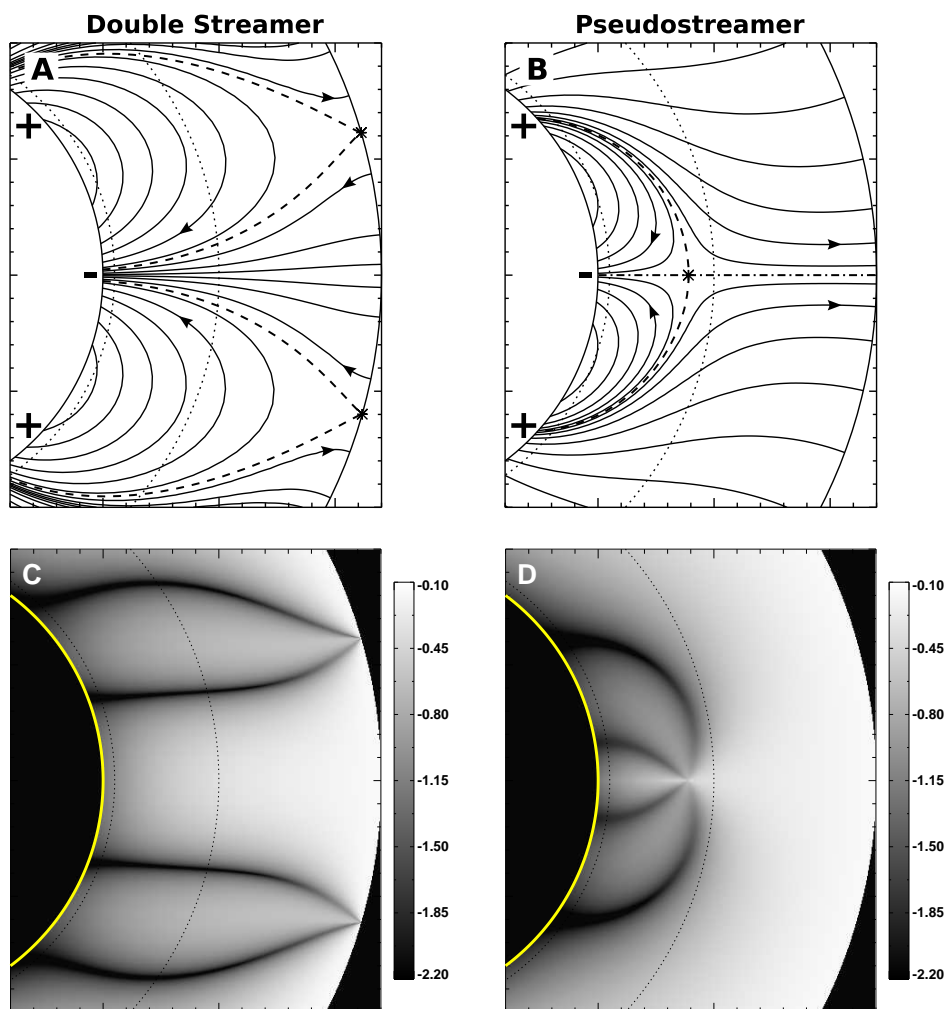


Fig. 1.— 2.5D axisymmetric models of a DS (A) and a PS (B) are shown with field line traces. Note that the field lines were chosen to illuminate topology and their density does not correspond to field strength. The nulls are marked with stars, and the separatrices as dashed or dash-dotted lines. The corresponding forward-modeled relative linear polarization, L/I , is shown below in (C), (D) in log scale with the field of view of the CoMP instrument, demarcated by the dotted lines.

2.1. Simulated coronal polarization

We use the axisymmetric models shown in Figure 1A and 1B to simulate coronal polarization, which is directly sensitive to the magnetic field in the corona. Figures 1C, and 1D show the line-of-sight integrated simulated relative linear polarization, $L/I = \sqrt{Q^2 + U^2}/I$, where I , Q , and U are the Stokes parameters of the emission from the Fe XIII transition at 10747 Å. This polarization is primarily due to the Hanle effect in the saturated regime¹.

Beginning with the magnetic configurations shown in Figures 1A, and 1B respectively, we used the FORWARD suite of codes (Judge et al. 2006; Gibson et al. 2010; Rachmeler et al. 2012, 2013) to generate simulated polarization images using a simple spherically symmetric hydrostatic temperature and density model (Gibson et al. 1999). The elongated dark features in these images mark the locations of the Van Vleck inversions – where the magnetic field is at $\sim 54^\circ$ from solar radial. A set of closed magnetic loops in the plane of the sky results in two elongated Van Vleck inversion lines where L approaches zero².

In most observations of coronal cavities on the limb, where the PIL is aligned with the line-of-sight, we see decreased L/I above the PIL due to field that is sheared or twisted into the line-of-sight (Bał-Stęślicka et al. 2013). Because the structures in our simple models do not contain azimuthal field, this decreased L/I is not present. For our analysis, we focus on the locations of the Van Vleck inversions, which are enough to distinguish between these two magnetic configurations.

¹For a more complete discussion of the Hanle effect in the saturated regime, see for example Casini & Judge 1999, Trujillo Bueno 2001, Casini 2002.

²For more information on interpreting linear polarization observations see Rachmeler et al. 2012 and references therein.

The differences between the L/I signatures of these two magnetic morphologies are clear. The DS (Figure 1C) shows two sets of roughly parallel Van Vleck inversions. Note that although they converge at the null line on the source surface, in the lower corona they are essentially parallel. This parallel nature is consistent with other observations of coronal cavities that overlie PILs when little or no line-of-sight field is present. (Rachmeler et al. 2013; Bąk-Stęślińska et al. 2013). In the PS, on the other hand, the Van Vleck inversions clearly converge at the null location. Although this specific convergence configuration is for unsheared arcades, the addition of shear still results in Van Vleck inversions that do not reach significantly higher than the separator. Thus, these two structures are easily identifiable in L/I observations provided that the separator is at low enough altitude to appear in the field-of-view, and the PILs are along the line-of-sight.

3. Observations

The observations presented here include data from the following instruments: PROBA2/SWAP 174 Å (PRoject for Onboard Autonomy 2/Sun Watcher using Active Pixel System detector and Image Processing; Seaton et al. 2013b; Halain et al. 2013); CoMP 10747 Å (Coronal Multichannel Polarimeter; Tomczyk et al. 2008) relative linear polarization (L/I); and ChroTel (Chromospheric Telescope; Bethge et al. 2011) $H\alpha$ 6563 Å. Since CoMP is a ground-based instrument, and only observes at specific times, we chose two CoMP observations to mark the times the DS (19:00 UT on 5 May 2013) and PS (19:30 UT on 10 May 2013) were visible on the western limb of the sun. These CoMP L/I observations are shown in Figures 3C and 3D. Simultaneously obtained SWAP observations are shown in Figures 3A and 3B.

The intensity observations in SWAP appear to show a topological transition from a DS to a PS. The DS structure is more ambiguous than the PS structure. The 10 May

observation clearly shows a cusp-shape void (near the ‘x’ in Figure 3B) above the two filament channels; bright structure is also clearly visible just outside the void. The bright features indicate that two domains of open field come together, and because this happens above two PIL’s, they are likely of the same polarity. Note that in Figure 3, the SWAP data is inverted, so bright emission is dark. This cusp structure is likely a temperature effect suggesting that the void contains plasma that is too hot to be seen by SWAP (Seaton et al. 2013a). In the 5 May data, there is no clear indication of open field between the cavities, but no cusp shape is visible.

The DS nature of the structure on 5 May is, however, clearly visible in the CoMP data (Figure 3C). The two sets of Van Vleck inversions are distinct and roughly parallel. This is very similar to the simulated emission from the analytical DS model (Figure 1C). It is interesting that these streamers do not have decreased L/I emission between the Van Vleck inversion, indicating that any sheared or twisted field is either entirely below the $1.05 R_{\odot}$ CoMP occulter or not present (Bałk-Stęślicka et al. 2013). The small size of the cavities in the corresponding SWAP image indicate that the former is likely.

The PS observation in CoMP (Figure 3D) is not as clear as the DS observation. There are several Van Vleck inversion lines that begin to converge like they do in Figure 1D but the convergence point (at or near the location of the ‘x’) is unfortunately located outside of the CoMP field-of-view. There are six elongated dark structures visible in Figure 3D. The uppermost and lowermost are located outside of the PS. The upper one is related to the edge-on loops seen in SWAP, and the lower is a noise artefact. The inner four are the Van Vleck inversions of the PS. The quality of the data was also better on 5 May than 10 May due to weather conditions.

For both dates, it is the *combination* of the SWAP and CoMP data that points to the transition from a DS to a PS structure. On 5 May, the CoMP data are clearly indicative of

a DS, which is consistent with the SWAP data although the SWAP data is ambiguous. On 10 May the cusp-shape in the SWAP observation is a clear sign of two open field domains coming together above two PILs, indicative of a PS morphology. The CoMP data supports this with the Van Vleck inversions being bent towards the location of the top of this cusp, although there are still strong ambiguities in the CoMP observations, most notably because the top of the PS lies above the CoMP field-of-view.

To determine the locations of the two filament channels, we used medianed high signal-to-noise SWAP data obtained on 30 April 2013 around 09:40 UT, when the filament channels were located on-disk. The longitudes at which the DS and PS were observed are indicated by the solid lines on the SWAP image in Figure 4. The filament channels appear as two elongated dark structures near the south pole (light in the inverted SWAP image), indicated by the dotted lines in Figure 4. $H\alpha$ observations from ChroTel reveal that neither channel is consistently filled with filament material.

The lack of clearly identifiable filament material makes it difficult to identify the location of both filament channels precisely. We used the standard PFSS extrapolation from 4 May 2013 at 12:04 UT from the SolarSoft PFSS package to confirm the existence of two continuous PILs. The extrapolation does indeed show two PILs with closed arcade structures above them.

The arcades increase in height from east to west along the channels, but do not open into two separate streamers on the west end where our observations show a DS. Indeed we would not necessarily expect to see a DS as PFSS extrapolations are potential and do not accurately model locations where electrical currents are important, such as near filaments. The inclusion of such currents along a PIL (resulting in sheared or twisted field) can cause an expansion of the overlying arcade compared to PFSS extrapolations. The strength of the currents can also vary along the PIL (Figure 3 by Yeates & Mackay 2012). The sheared

field would increase the magnetic pressure, and thus the outward-directed magnetic force, while the inward tension force from the overlying arcade would remain the same. Thus, the equilibrium magnetic configuration is inflated when shear or twist are introduced to the system.

Furthermore, the open/closed field boundaries are strongly dependent on the height of the source surface, the standard height being $2.5 R_{\odot}$. However, depending on the solar activity, a source surface as low as $1.5 R_{\odot}$ may best fit the observations (Lee et al. 2011). Lowering the source surface has the effect of increasing the size of the open field domains and could also easily result in open field between two large arcades. Thus, the lack of a DS in the PFSS model does not preclude the presence of a DS in the true corona.

Between May 5 and 10, there are two eruptions involving the lower filament channel. The first eruption occurs at roughly 7 May 01:20-21:45 UT and the second at 9 May 02:45-13:45 UT. Both occur primarily in the PS section of the structure. Neither disrupts the underlying morphology of the hybrid system except temporarily during the eruption itself.

4. Discussion

In this letter we have presented an observation and a simplified model of a single hybrid magnetic structure containing both a side-by-side double-streamer (DS) and a pseudostreamer (PS) along two continuous filament channels. This morphological change is supported by a combination of SWAP EUV images and CoMP linear polarization measurements. While previous studies (Dove et al. 2011; Bał-Stęślicka et al. 2013; Rachmeler et al. 2013) have considered the coronal polarization signatures of streamers, this letter presents the first research on coronal polarization characteristics of PSs.

The CoMP data from 5 May 2013 (Figure 3C) is consistent with a DS structure, with

two sets of roughly parallel Van Vleck inversion lines, much like those shown in our analytic model (Figure 1C). Several days later, SWAP sees a cusp-shape where two open field domains come together above two PILs, which is a good indication of a PS. The CoMP data from that time shows two sets of Van Vleck inversion lines that begin to converge on a location above upper boundary of CoMP (Figure 3D). This characteristic convergence towards the PS null or separator is predicted by the FORWARD model for a PS (Figure 1D).

Despite the absence of continuous filament material over the full extent of both channels (Figure 4), PFSS extrapolations confirm the presence of two continuous PILs. The combination of observations and models presented here point to a single hybrid structure containing both DS and PS magnetic morphologies.

The solar wind from streamers is generally thought to be slow wind (Gosling et al. 1981; Strachan et al. 2002), while there is some debate about the nature of the wind from that originates in and around pseudostreamers (Wang et al. 2007; Riley & Luhmann 2012; Wang et al. 2012; Panasenco & Velli 2013). As a result, as the hybrid structure rotates across the solar disk, the transition from a DS to a PS may influence the characteristics of the solar wind between the Sun and the Earth.

The open field at the center of the DS produces fast solar wind, while the two streamers produce slow wind. The three streams may interact in interesting ways once they reach the heliosphere, implying that the solar wind from the DS alone could have complex structure.

Furthermore, reconnection in a helmet streamer occurs primarily in the current sheet, while reconnection in the PS occurs primarily at the separator. Because the reconnection in the PS occurs at a lower height, and it is likely that the composition of the solar wind originating from the two regions is different.

The change in magnetic configuration could also affect the stability of the enclosed

filament. The lower height of the separator in the PS structure likely results in a more rapid decrease in field strength with height. This may reduce the height of the critical value of the decay index, which determines the filament’s vulnerability to eruption via torus instability (Kliem & Török 2006; Démoulin & Aulanier 2010; Zuccarello et al. 2012). Török et al. (2011), Titov et al. (2012), and Lynch & Edmondson (2013) have also shown that an eruption in one of the lobes of a PS can easily trigger a sympathetic eruption in the other lobe. Thus these hybrid structures may be more vulnerable to eruption than streamers or double streamers alone.

Although this letter presents the first identification of this type of hybrid structure, we do not believe they are an uncommon phenomenon. Especially near solar maximum, when there are multiple polar crown filaments (Mouradian & Soru-Escaut 1994; Minarovjech et al. 1998) that are slowly driven together due to the meridional flow, there is the potential for similar structures to form. More work is needed to find further instances of such structures, analyze their 3D topology in detail, and investigate their heliospheric implications.

D.B.S. and L.A.R. acknowledge support from the Belgian Federal Science Policy Office (BELSPO) through the ESA-PRODEX program, grant No. 4000103240. S.J.P. acknowledges the financial support of the Isle of Man Government. The authors would like to thank Francesco Zuccarello, Sarah Gibson, Duncan Mackay, and Clare Parnell for helpful discussions. SWAP is a project of the Centre Spatial de Liege and the Royal Observatory of Belgium funded by BELSPO. CoMP data is provided courtesy of the Mauna Loa Solar Observatory, operated by the High Altitude Observatory (HAO), as part of the National Center for Atmospheric Research (NCAR). NCAR is supported by the National Science Foundation. ChroTel is operated by the Kiepenheuer-Institute for Solar Physics (KIS), at the Spanish Observatorio del Teide.

Facilities: PROBA2, STEREO, SDO

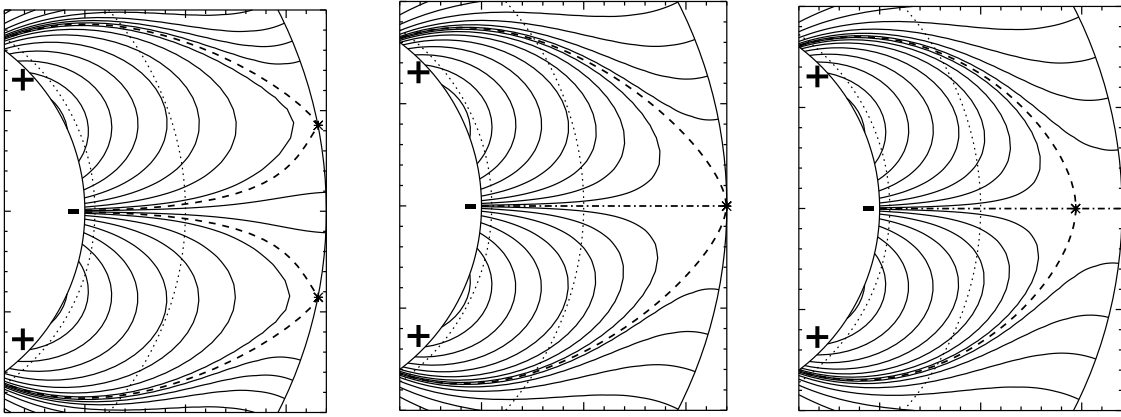


Fig. 2.— A cartoon showing the transition between DS (left) and PS (right) morphologies as longitudinal slices. Stars denote the location of the nulls. Field line density does not correspond to field strength. This figure is available as an animation in the electronic edition of the *Astrophysical Journal*.

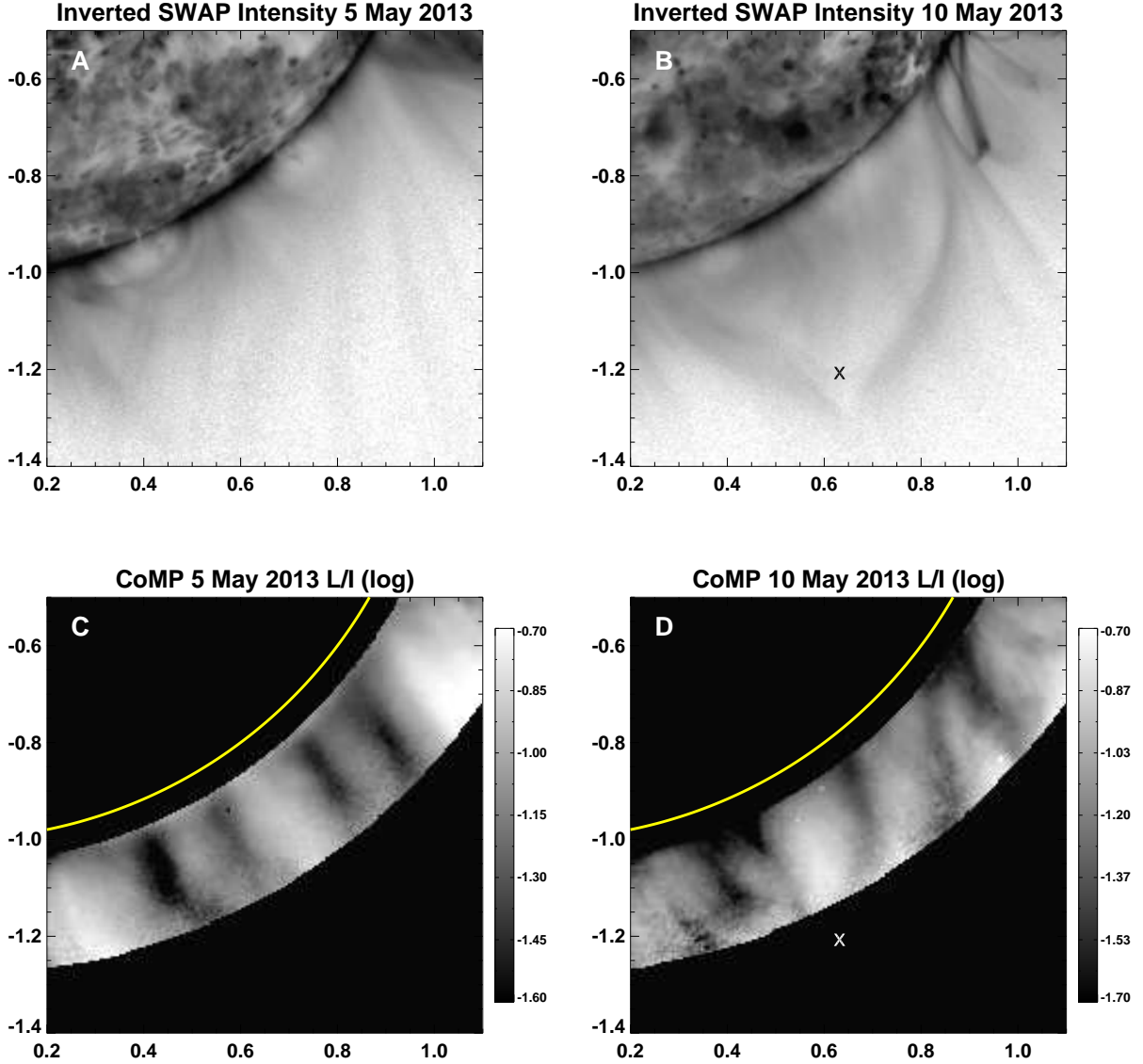
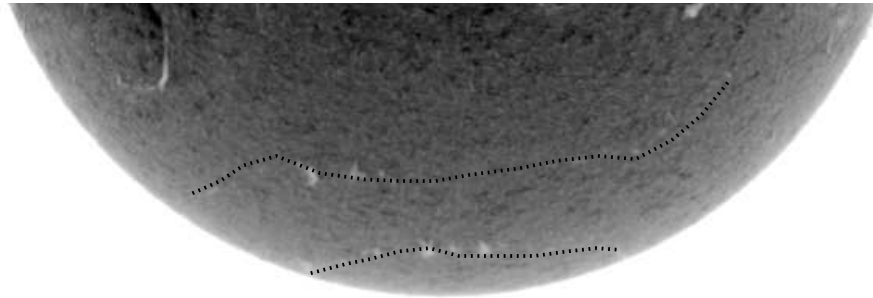
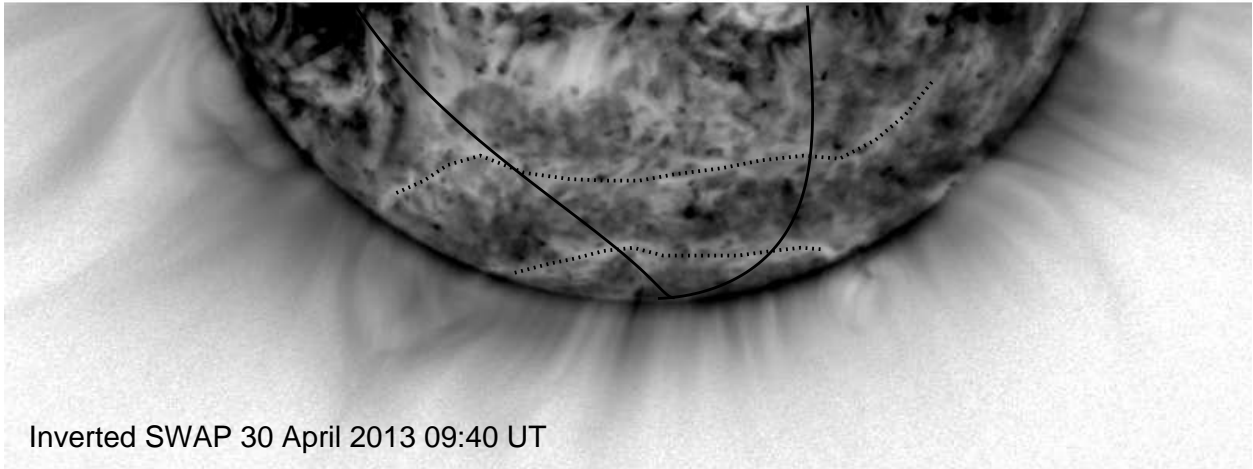


Fig. 3.— Inverted SWAP (upper) and CoMP (lower) observations of the unified structure as a DS on 5 May 2013 (left), and a PS on 10 May 2013 (right). The ‘x’ in B and D shows the approximate separator location for the PS. All length units are in R_{\odot} from disk center. The SWAP images are available as an animation in the electronic edition of the *Astrophysical Journal*.



Inverted ChroTel 30 April 2013 09:39 UT



Inverted SWAP 30 April 2013 09:40 UT

Fig. 4.— Inverted SWAP and ChroTel observations showing the two filament channels, which are traced with dotted lines. The solid lines show the de-rotated longitudes of the DS and PS as observed by CoMP on 5 May 2013 (right line) and 10 May 2012 (left line).

REFERENCES

- Bethge, C., Peter, H., Kentischer, T. J., et al. 2011, *A&A*, 534, A105
- Bąk-Stęślička, U., Gibson, S. E., Fan, Y., et al. 2013, *ApJ*, 770, L28
- Casini, R. 2002, *ApJ*, 568, 1056
- Casini, R., & Judge, P. G. 1999, *ApJ*, 522, 524
- Démoulin, P., & Aulanier, G. 2010, *ApJ*, 718, 1388
- Dove, J. B., Gibson, S. E., Rachmeler, L. A., Tomczyk, S., & Judge, P. 2011, *ApJ*, 731, L1
- Gibson, S. E., Fludra, A., Bagenal, F., et al. 1999, *J. Geophys. Res.*, 104, 9691
- Gibson, S. E., Kucera, T. A., Rastawicki, D., et al. 2010, *ApJ*, 724, 1133
- Gosling, J. T., Asbridge, J. R., Bame, S. J., et al. 1981, *J. Geophys. Res.*, 86, 5438
- Halain, J.-P., Berghmans, D., Seaton, D. B., et al. 2013, *Sol. Phys.*, 286, 67
- Judge, P. G., Low, B. C., & Casini, R. 2006, *ApJ*, 651, 1229
- Kliem, B., & Török, T. 2006, *Physical Review Letters*, 96, 255002
- Lee, C. O., Luhmann, J. G., Hoeksema, J. T., et al. 2011, *Sol. Phys.*, 269, 367
- Lynch, B. J., & Edmondson, J. K. 2013, *ApJ*, 764, 87
- Minarovjeh, M., Rybansky, M., & Rusin, V. 1998, *Sol. Phys.*, 177, 357
- Mouradian, Z., & Soru-Escaut, I. 1994, *A&A*, 290, 279
- Panasenco, O., & Velli, M. 2013, in *American Institute of Physics Conference Series*, Vol. 1539, *American Institute of Physics Conference Series*, ed. G. P. Zank, J. Borovsky,

- R. Bruno, J. Cirtain, S. Cranmer, H. Elliott, J. Giacalone, W. Gonzalez, G. Li, E. Marsch, E. Moebius, N. Pogorelov, J. Spann, & O. Verkhoglyadova, 50–53
- Parnell, C. E., Haynes, A. L., & Galsgaard, K. 2008, *ApJ*, 675, 1656
- Pneuman, G. W., & Kopp, R. A. 1971, *Sol. Phys.*, 18, 258
- Rachmeler, L. A., Casini, R., & Gibson, S. E. 2012, in *Astronomical Society of the Pacific Conference Series*, Vol. 463, *Second ATST-EAST Meeting: Magnetic Fields from the Photosphere to the Corona.*, ed. T. R. Rimmele, A. Tritschler, F. Wöger, M. Collados Vera, H. Socas-Navarro, R. Schlichenmaier, M. Carlsson, T. Berger, A. Cadavid, P. R. Gilbert, P. R. Goode, & M. Knölker, 227
- Rachmeler, L. A., Gibson, S. E., Dove, J. B., DeVore, C. R., & Fan, Y. 2013, *Sol. Phys.*, doi:10.1007/s11207-013-0325-5
- Riley, P., & Luhmann, J. G. 2012, *Sol. Phys.*, 277, 355
- Seaton, D. B., De Groof, A., Shearer, P., Berghmans, D., & Nicula, B. 2013a, *ApJ*, 777, 72
- Seaton, D. B., Berghmans, D., Nicula, B., et al. 2013b, *Sol. Phys.*, 286, 43
- Strachan, L., Suleiman, R., Panasyuk, A. V., Biesecker, D. A., & Kohl, J. L. 2002, *ApJ*, 571, 1008
- Titov, V. S., Mikic, Z., Török, T., Linker, J. A., & Panasenco, O. 2012, *ApJ*, 759, 70
- Tomczyk, S., Card, G. L., Darnell, T., et al. 2008, *Sol. Phys.*, 247, 411
- Török, T., Panasenco, O., Titov, V. S., et al. 2011, *ApJ*, 739, L63
- Trujillo Bueno, J. 2001, in *Astron. Soc. Pac.*, Vol. CS-236, *Advanced Solar Polarimetry – Theory, Observation, and Instrumentation*, ed. M. Sigwarth, 161

Wang, Y.-M., Grappin, R., Robbrecht, E., & Sheeley, Jr., N. R. 2012, ApJ, 749, 182

Wang, Y.-M., Sheeley, Jr., N. R., & Rich, N. B. 2007, ApJ, 658, 1340

Yeates, A. R., & Mackay, D. H. 2012, ApJ, 753, L34

Zuccarello, F. P., Romano, P., Zuccarello, F., & Poedts, S. 2012, A&A, 537, A28